https://doi.org/10.5194/egusphere-2026-4249
Preprint. Discussion started: 17 August 2026

Isotope-enabled modeling of fast streamflow dynamics in a steep Alpine catchment

Harsh Beria[1,2], Lionel Benoit[3], Grégoire Mariethoz[4], Natalie C. Ceperley[5], Bettina Schaefli[5]

[1] Department of Civil, Environmental and Geomatic Engineering, ETH Zurich, Zurich, Switzerland
[2] WSL Institute for Snow and Avalanche Research SLF, Davos, Switzerland
[3] Biostatistics and Spatial Processes (BioSP), INRAE, 84914 Avignon CEDEX 9, France
[4] Institute of Earth Surface Dynamics (IDYST), University of Lausanne (UNIL), Switzerland
[5] Institute of Geography (GIUB), and Oeschger Center for Climate Change Research (OCCR), University of Berne, Switzerland

Correspondence to: Harsh Beria (hberia@ethz.ch)

Abstract. Alpine headwater catchments often produce streamflow peaks anywhere from minutes to hours after a rainfall event, quickly mobilizing previously stored subsurface water. Understanding and describing this response to rainfall events and its variations via modeling remains challenging, despite the growing availability of data, including tracer data such as stable isotopes of water, to inform internal flow partitioning.

Here, we present a novel flux partitioning routine integrated into an existing hydrological model based on the Geomorphological Instantaneous Unit Hydrograph and multiple subsurface reservoirs. The model structure is based on a detailed perceptual model derived from available field data, and it simulates streamflow magnitude and streamwater isotopic ratios at high temporal resolution (10-minute intervals) in a snow-dominated headwater catchment in the western Swiss Alps (Vallon de Nant) over two consecutive summers. By jointly calibrating the model with both streamflow quantity and streamwater isotopic ratios, we obtain a reliable representation of catchment-scale partitioning of streamflow between groundwater, snowmelt, and direct runoff. The simulations showed that despite the catchment's high level of flashiness, with peak streamflow occurring within an hour of peak rainfall, most streamflow originates from subsurface flow pathways with limited contributions from direct runoff. Even during short periods of intense convective rainfall events, peak flows mostly comprise water released by subsurface storage, which are mobilized by rainfall.

Our results show that incorporating stable water isotopes into a relatively simple catchment-scale model can refine model structure, reduce parameter uncertainty, and improve process attribution of short-timescale streamflow generation dynamics. We discuss the advantages and limitations of the proposed isotope-enabled modeling approach and its potential extension to other catchments and year-round modeling.

1. Introduction

The last decade of research has significantly advanced our understanding of catchment-scale streamflow generation dynamics and their representation in hydrological models (Peters-Lidard et al., 2019). Such models enable predictions of future water resources, essential to gauge the impacts of climate change on different facets of the water cycle. This is becoming increasingly urgent as climatic extremes such as floods and droughts become more frequent (Stott, 2016), and as subsequent changes in precipitation regimes impacts ecosystem functioning with full circle repercussions on the water cycle (Malhi et al., 2020).

Most hydrological models are calibrated primarily against streamflow timeseries at the catchment outlet, because streamflow presents a catchment-scale integrated signal and is widely available (Hrachowitz et al., 2016). However, streamflow-only calibration can limit the reliability of such models, sometimes leading to the right answers (i.e. matching streamflow hydrographs) but for the wrong reasons (Kirchner, 2006), e.g., by underestimating evaporation compensated by higher soil moisture in the model domain (Sutanudjaja et al., 2014). This problem mainly arises because the model incorrectly simulates the internal flux partitioning (e.g., between evapotranspiration, groundwater recharge, and discharge), allowing multiple parameterizations to yield similar streamflow performance (Hrachowitz and Clark, 2017; Jung et al., 2025; Popp et al., 2025). The reliability of internal model states can be improved by using additional observations such as remote-sensing based estimates of evapotranspiration (Dembélé et al., 2020a; Odusanya et al., 2019; Rajib et al., 2018), snow cover (Nijzink et al., 2018; Parajka and Blöschl, 2008; Salvatore et al., 2018), terrestrial water storage (Bai et al., 2018; Dembélé et al., 2020b), and soil moisture (Kunnath-Poovakka et al., 2016; Sutanudjaja et al., 2014). Such additional observations can constrain simulated storages and fluxes, but do not necessarily resolve the distinction between water transport and rainfall-streamflow response.

This distinction is commonly framed in terms of water velocity and hydrological celerity. Celerity describes the speed at which a streamflow response to rainfall or snowmelt propagates through a catchment, whereas velocity refers to the speed at which an individual water particle traverses the catchment (Mcdonnell and Beven, 2014). Streamflow observations primarily constrain the timing and magnitude of the catchment response and provide information on celerity, which in many conceptual models is governed by storage and connectivity thresholds (Harman, 2019; Mcdonnell and Beven, 2014). However, streamflow observations alone provide much weaker constraints on water velocities, which depend on storage volumes, mixing processes, and the partitioning of water among diverse flow pathways.

Environmental tracers such as stable water isotopes can reduce this ambiguity because they allow tracing of water molecules through the hydrological cycle, and provide information on water sources, storage volumes, mixing processes, flow pathways, and storage-discharge relationships (Jung et al., 2025). Model calibration with streamflow quantity and streamwater isotopes can therefore extend beyond classical celerity-based calibration of hydrological models. This distinction is particularly important in steep alpine catchments, where rainfall can generate streamflow peaks within minutes to hours (Brunner et al., 2018; Stoffel et al., 2016; Weingartner et al., 2003), even though most streamwater may originate from water stored in the catchment before the event (Kirchner, 2003; Klaus and McDonnell, 2013; Obradovic and Sklash, 1986; Pearce et al., 1986; Popp et al., 2025). In such settings, rainfall or snowmelt may mobilize older groundwater stored within a catchment rather than directly contributing to streamflow as event water.

This interpretation is supported by a long history of isotope-based hydrograph separation studies showing that pre-event water dominates stormflow across diverse landscapes, ranging from the Appalachians and the Rocky Mountains in the USA (Dewalle et al., 1988; Frisbee et al., 2011) , the Maimai catchment in New Zealand (Weiler et al., 2003),

https://doi.org/10.5194/egusphere-2026-4249
Preprint. Discussion started: 17 August 2026

to steep Swiss headwaters (von Freyberg et al., 2018). We point readers to Section 4.2.1.3 in the review from Popp et al. (2025) for an exhaustive list of such studies.

Recent advances in isotope-enabled hydrological modeling have significantly improved ecohydrological modeling, moving beyond calibration based on hydrometric data alone (Birkel et al., 2020; van Huijgevoort et al., 2016; Knighton et al., 2020; Nan and Tian, 2024; Piovano et al., 2019; Snarski et al., 2025; Stadnyk and Holmes, 2020; Tunaley et al., 2017; Watson et al., 2023). Approaches span a wide range of complexity and spatial resolutions, ranging from extension of conceptual modeling approaches with storage selection functions (Benettin et al., 2017; Knighton et al., 2019) to spatially distributed energy-balance models (Kuppel et al., 2018; Müller et al., 2025). Many isotope modeling frameworks (e.g., THREW-T, IsoWATFLOOD, WATET, STARR/STARR-tropic, J2000-iso, EcH2O-iso) have been applied at varied spatial scales, ranging from small headwater catchments to larger domains (see review from Jung et al., (2025)).

Despite this progress, applications of isotope-enabled hydrological models in snow-dominated, high-relief alpine catchments remain limited (Müller et al., 2025). This is a critical gap because these environments are undergoing rapid cryospheric changes under enhanced global warming (Pepin et al., 2015, 2022). In alpine headwater catchments, intense convective rainfall during summers generates fast streamflow responses (von Freyberg et al., 2018; Michelon et al., 2021), which can be interpreted as evidence for the fast transfer of rainfall to the stream through infiltration-excess or saturation-excess overland flows (Mcdonnell and Beven, 2014). Stable water isotopes provide a means to test this interpretation by disentangling streamflow into groundwater vs event-water at the catchment-scale.

In this article, we use stable water isotopes to parameterize the dominant streamflow-generation processes during two successive summers in Vallon de Nant, a high-relief alpine catchment in western Switzerland. We develop a hydrological model based on spatially distributed Geomorphological Instantaneous Unit Hydrograph and multiple subsurface reservoirs to estimate streamflow at 10-minute interval during two consecutive summer periods, when reliable observations of spatially distributed rainfall fields were available. A flux partitioning routine is implemented in the model to also simulate streamwater isotopic ratio at 10-minute interval. Isotope measurements from a two-year intensive monitoring campaign across multiple hydrological fluxes are used to constrain the isotopic composition of the different model compartments, building on earlier studies of the catchment's hydrological functioning (Beria et al., 2020; Michelon et al., 2023). Model parameters are jointly calibrated using streamflow quantity and streamwater isotopes. The key objectives are to: (1) understand streamflow generation processes in this alpine headwater catchment, (2) reproduce streamflow and its isotopic dynamics at 10-minute temporal resolution during two consecutive summer periods, and (3) quantify the contribution of direct flow, snowmelt, and groundwater to summer streamflow generation.

2. Study area

2.1 Topography, geomorphology, geology

Vallon de Nant is a headwater catchment located in the Vaud Alps in western Switzerland (Figure 1a). Stretching across an area of 13.4 km^2, catchment elevation ranges from 1253 m to 3051 m a.s.l. (mean 2012 m a.s.l.). Vallon de Nant has a protected status (Natural Reserve of the Muveran) since 1969 and is one of the few relatively unperturbed

https://doi.org/10.5194/egusphere-2026-4249
Preprint. Discussion started: 17 August 2026

alpine catchments in Switzerland (Michelon et al., 2021). Steep and large slopes form ~63.6% of the catchment area, with mean catchment slope of around 36° (Thornton et al., 2018). Forests cover approximately 14% of the catchment area and consist of dense stands dominated by *Picea abies* (Norway spruce) at lower elevations, transitioning to active pastures and open forest dominated by *Larix decidua* (Larch) at mid-elevations. Floodplains and talus span from lower to mid-elevation levels and form 12.3% and 6% of the catchment area. In the South-western tip of the catchment, there is a small glacier occupying ~4.4% of the catchment area.

The catchment comprises several geomorphological units, including steep limestone cliffs on the eastern ridge with ephemeral stream networks, flysch cliffs with grassy slopes and well-developed soils along the western ridge, a riparian wetland, and moraine deposits in the upper valley. Shallow silty loam soils have developed on moraine deposits, screes, and landslides (Eeckman et al., 2025). Long-term ecosystem monitoring has enabled and motivated several recent studies of surface and subsurface hydrological processes in Vallon de Nant (Beria et al., 2020; Eeckman et al., 2025; Michelon et al., 2021, 2023; Thornton et al., 2022).

Vallon de Nant experiences a typical European alpine climate, with precipitation mostly originating from the North Atlantic Ocean, followed by the Mediterranean, the European land surface and the North and Baltic seas (Sodemann and Zubler, 2010). Annual precipitation amounts to ~1900 mm with snowfall accounting for 40-45% of annual precipitation (Beria et al., 2020). The mean annual air temperature is 1.8°C.

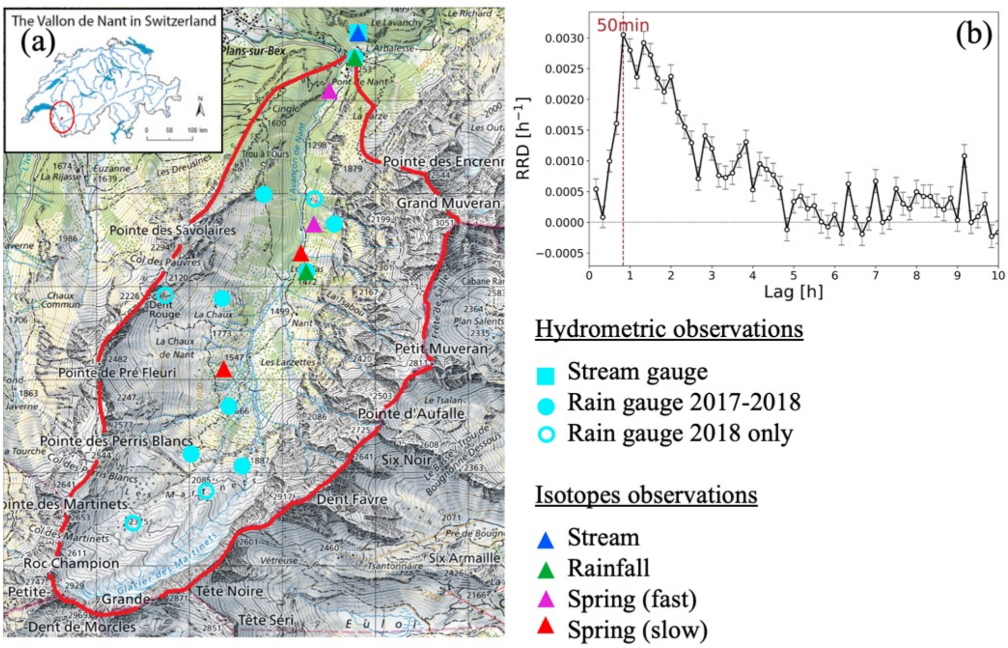

Figure 1: (a) Map showing Vallon de Nant along with various monitoring sites for rain, spring and stream waters and their isotopic ratios, (b) runoff response distribution for Vallon de Nant calculated using ensemble rainfall-runoff analysis (Kirchner, 2024).

https://doi.org/10.5194/egusphere-2026-4249
Preprint. Discussion started: 17 August 2026

2.2 Monitoring data

During the summers of 2017 and 2018 (July to September), a spatially dense network of drop-counting rain gauges called Pluvimates (www.driptych.com) were installed in 8 (2017) to 12 (2018) different locations within Vallon de Nant (Figure 1). Pluvimates record rainfall at 0.01 mm resolution and were setup at a 2-minute temporal frequency (Benoit et al., 2018; Michelon et al., 2021). For this study, rainfall data were aggregated to 10-minutes temporal resolution and point measurements were interpolated to 300-m spatial resolution using a Thiessen Polygon approach (Schumann, 1998). Due to the remote catchment location, substantial snow accumulation, and the absence of heated rain gauges, Pluvimates could only be installed and maintained during continuous snowfall-free periods, restricting hydrological modeling using their data to July-September in 2017 and 2018.

Stream water level was continuously measured at the catchment outlet (Figure 1a) at 1-minute temporal frequency using a sonar-based stream gauge installed on top of a weir (Michelon et al., 2023). Streamflow was estimated using a rating curve based on 23 salt discharge measurements (Ceperley et al., 2018). For this study, streamflow was aggregated to 10-minute temporal resolution.

During the years 2017 and 2018, Vallon de Nant was extensively monitored for stable water isotopes in rainfall, snowpack, streamflow, and springs (Michelon et al., 2023). Rainfall was sampled bi-weekly at two locations, with one site located next to the catchment outlet and the other in the middle part of the catchment on a tributary (Figure 1a). Rainfall was collected using a 13 cm diameter plastic funnel that led into a 2.5L insulated screw-top low-density polyethylene (LDPE) plastic bag. Once every two weeks, the plastic bag was weighed, mixed, and emptied into 12 ml amber borosilicate glass vials, which were kept in cool conditions until subsequent analysis in the laboratory.

Grab snow samples from snow pits at two different locations were collected during the winters of hydrologic years 2017 and 2018. We relied on snowpack samples as deploying snowmelt lysimeters was not feasible due to the harsh weather conditions and frequent avalanches during winters, limiting access to the catchment. The collected snow was sealed in 700 ml zip bags made from 120µm biaxially oriented polypropylene and LPDE plastic. The sealed snow samples were melted at ambient air temperature, and a subsample of well-mixed meltwater was taken in 12 ml amber borosilicate glass vial from each bag.

An automatic Teledyne ISCO 6712C compact portable sampler with 24 bottles with 500 ml storage capacity was installed at the catchment outlet during the summers of 2017 and 2018, collecting stream samples at 6-12 hourly temporal frequency. The automatic sampler was programmed to fill the bottles to about half of their capacity. Due to low air temperatures, minimal evaporation was seen in the stream water samples throughout the measurement period. Spring isotope samples were collected bi-weekly at five different locations in 12 ml borosilicate glass vials.

A Cavity Ring Down Spectrometer (CRDS) system (Picarro L2140-i) was used to measure the stable isotope composition of waters in precipitation, streamwater, and springs using the δ notation (δ^2H, $\delta^{18}O$). Samples were injected between 6 and 8 times with the first three injections being discarded to avoid memory effects (Michelon et al., 2023). The stable water isotopes values were standardized against three internal standards (ANZO, EMEB, SAAS), these standards were regularly calibrated against the Vienna Standard Mean Ocean Water (VSMOW). The median analytical errors are 0.4‰ for δ^2H and 0.04‰ for $\delta^{18}O$. More details about the isotope measurements are available in Michelon et al., (2023).

https://doi.org/10.5194/egusphere-2026-4249
Preprint. Discussion started: 17 August 2026

3. Perceptual model of streamflow dynamics

The perceptual model for streamflow generation in Vallon de Nant is developed from high-resolution hydrometeorological observations, stable water isotope measurements in precipitation, snowpack, streamwater and springs, spring temperature dynamics, and previous field investigations in the catchment. The 10-minute streamflow observations indicate that peak streamflow typically occurs within approximately 50 minutes of rainfall peaks during summer (Figure 1b; also see Michelon et al., 2021). For context, only 9 out of 516 catchments analyzed across the United States had a time to peak shorter than 1 hour (Li et al., 2026), indicating that streamflow in Vallon de Nant responds quickly to rainfall. However, this rapid streamflow response alone does not indicate whether streamflow is generated by rapid event-water transfer or by rapid mobilization of water stored in the subsurface.

The isotope observations provide constraints on this ambiguity. Streamwater and groundwater had similar isotopic ratios, lay between rainfall and snowpack isotopic signature, and were strongly dampened relative to precipitation isotopes (Figure 2). This indicates that streamflow integrates rainfall- and snowmelt-derived water after substantial catchment storage and mixing, consistent with catchments acting as low-pass filters of the precipitation isotope signal (Kirchner et al., 2023). Groundwater showed slightly lower isotopic variability than streamwater, while both streamwater and groundwater were biased toward isotopically depleted, snowpack-like signature (Beria et al., 2020). Streamwater, groundwater, rainfall and snowpack isotopic ratios plotted close to the local meteoric water line (Figure 2), suggesting no significant evaporation- or sublimation-induced fractionation. Consequently, isotope fractionation during evaporation or sublimation is not represented in the model.

Rainfall and snowpack were isotopically distinct, with rainfall more enriched in heavier isotopes than snowpack, reflecting seasonal differences in condensation conditions and air-mass trajectories (Akers et al., 2017; Friedman et al., 1964). These differences allow rainfall and snowmelt to be treated as distinct isotopic inputs. Snowfall accounts for 40-45% of annual precipitation in Vallon de Nant, and the influence of snowmelt was visible in streamwater isotopes during spring (Figure 3). In May and June 2017 and 2018, streamwater was more depleted in heavier isotopes than in August and September, consistent with larger snowmelt contributions during the main melt period.

Most of the seasonal snowpack had disappeared from large parts of the catchment by the end of June in 2017 and 2018 (see Figure 5 in the work of Michelon et al., 2023), but residual snow can persist into summer in specific high-elevation terrain, particularly near ridges and mountain tops, below steep rockwalls in the south-eastern part of the catchment, and in shaded areas which receive lower incoming radiation. This melt pulse was visible in the diel fluctuations in streamflow in early July 2017 (Figure 4), likely sustained by snowmelt contributions from high-elevation snow patches. These diel streamflow fluctuations were missing in July 2018, consistent with earlier and faster snowmelt in 2018 (Michelon, 2022). We conceptualize the late-season snowmelt as originating mainly from the steep landscape units, where meltwater is rapidly transferred toward the stream network through coarse deposits that connect the rockwalls to the stream. In this conceptualization, residual late-season snowmelt contributes to streamflow without modifying the catchment-scale subsurface isotope composition, in contrast to the main seasonal snowmelt period, when meltwater recharges subsurface storages. Including this residual snowmelt flux was essential to reproduce the depleted streamwater isotope signal in early July, and the subsequent enrichment in streamwater from July to September (Figure 4). Because our simulations focus on July-September after most seasonal snow has disappeared,

https://doi.org/10.5194/egusphere-2026-4249
Preprint. Discussion started: 17 August 2026

we represent residual snowmelt with a simplified nonlinear storage-discharge model rather than a full snow accumulation, redistribution, and energy-balance melt model.

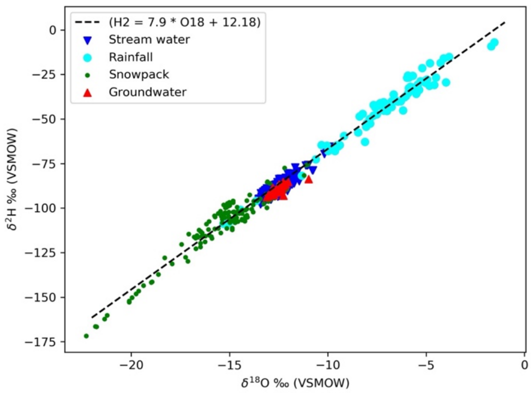

Figure 2: The local meteoric water line of Vallon de Nant showing the relationship between δ^2H and $\delta^{18}O$ in rainfall, snowpack, groundwater, and streamwater.

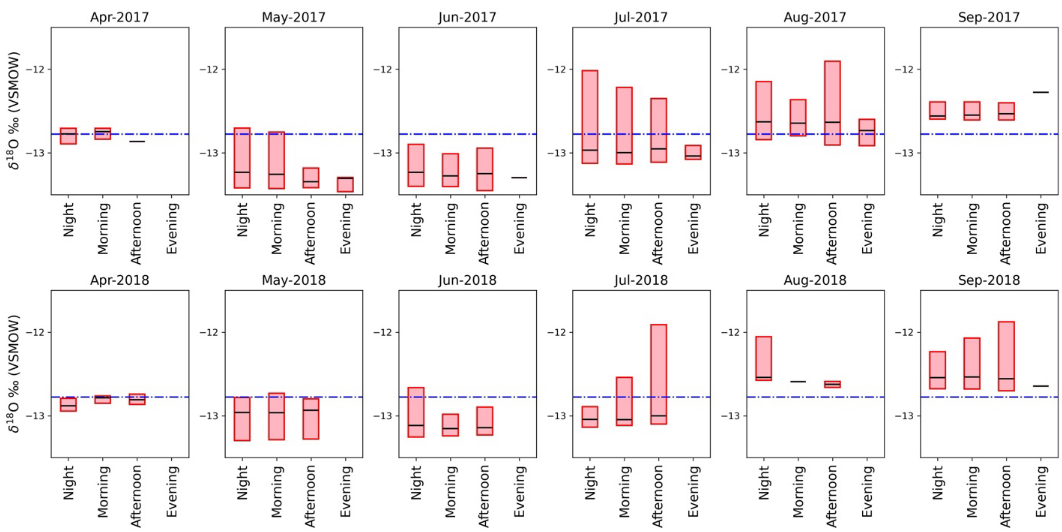

Figure 3: Diel variation in monthly streamwater $\delta^{18}O$ from April to September for 2017 and 2018. Each day is divided into 6-hour blocks: night (00:00 to 6:00), morning (6:00-12:00), afternoon (12:00-18:00) and evening (18:00-23:59). Boxes show the 5th to 95th percentile range of streamwater $\delta^{18}O$ values within each time block, and the central black line indicates the median. The blue dashed line represents the average streamwater $\delta^{18}O$ over the two hydrologic years.

https://doi.org/10.5194/egusphere-2026-4249
Preprint. Discussion started: 17 August 2026

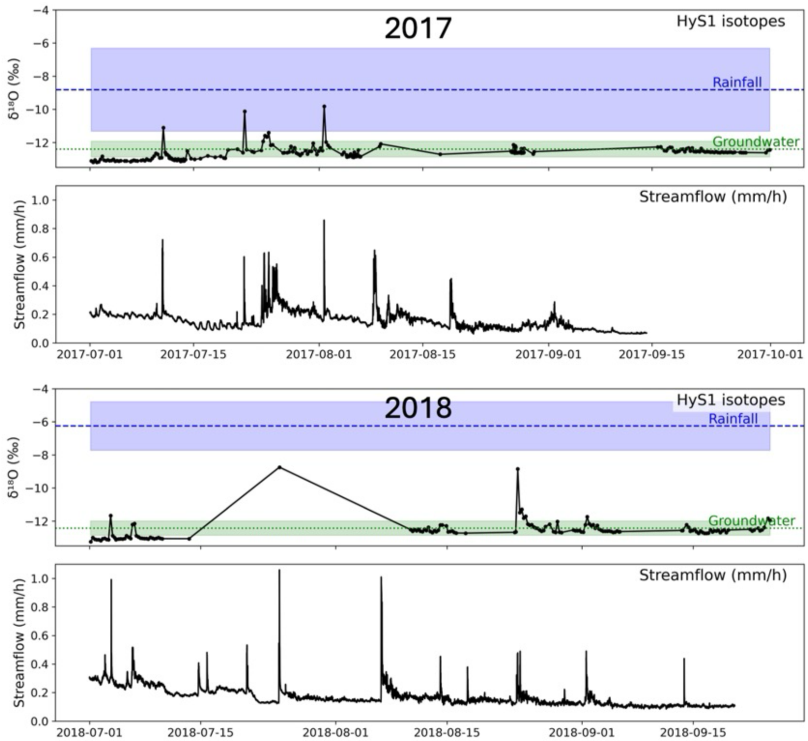

Figure 4: Observed streamflow and $\delta^{18}O$ dynamics in rainfall, groundwater, and streamwater at the outlet from July to September in 2017 and 2018. Rainfall and groundwater $\delta^{18}O$ are shown as year-specific means across sampling locations, with shaded region indicating ± one standard deviation. Streamflow is averaged over 10-minute intervals, while streamwater $\delta^{18}O$ values represent the isotopic ratio of streamwater samples collected at the outlet.

Glacier melt is not represented as a separate model component. In glacier-influenced alpine streams, daytime ice melt during peak summer can increase the contribution of isotopically depleted meltwater to streamflow and can produce diel depletion in streamwater isotopes (Beria et al., 2018; Müller et al., 2025). Such diel isotope patterns were not observed in Vallon de Nant during the summers of 2017 and 2018 (Figure 3), consistent with previous field evidence of negligible glacial-melt contributions to summer streamflow (Ceperley et al., 2020; Michelon et al., 2023).

From July to September, streamwater progressively became more enriched in heavier isotopes, indicating a declining influence of snowmelt and increasing influence of summer rainfall and groundwater contributions (Figure 4). Rainfall events produced rapid, but short-lived changes in streamwater isotopic ratio. During intense rainfall events, streamflow increases often coincided with sharp enrichment in streamwater $\delta^{18}O$ toward rainfall-like isotopic values. After these events, streamwater $\delta^{18}O$ returned toward groundwater-like values within 6-24 hours, depending on storm magnitude and duration (Figure 4). This rapid but transient isotopic response in streamwater indicates that rainfall contributes to event-scale streamflow dynamics, but the subsequent recovery toward groundwater isotopic ratio suggests that subsurface storage remains the dominant source of streamflow shortly after event peaks. During low flow periods in both years, streamwater $\delta^{18}O$ remained close to groundwater $\delta^{18}O$, highlighting the dominant role of groundwater discharge in sustaining baseflow.

https://doi.org/10.5194/egusphere-2026-4249
Preprint. Discussion started: 17 August 2026

Spring temperature dynamics, reported in a previous publication (Michelon et al., 2023), indicate two dominant subsurface flow pathways. Amongst the five sampled springs, three showed pronounced diel temperature fluctuations, whereas two showed strongly damped variations (see Figure 3 and Tables 1 and 2 in Michelon et al., 2023). We therefore represent groundwater discharge using two components: (1) a fast component representing shallow subsurface flow paths, and (2) a slower component representing deeper flow paths that sustain summer low flows. Accordingly, the model includes two subsurface storages, generating fast and slow groundwater discharge through nonlinear and linear storage-discharge relationships, respectively.

4. Hydrological model

4.1 Model structure

Based on the perceptual model described above, we develop a catchment-scale hydrological model that represents streamflow as the sum of direct flow, snowmelt, soil-water drainage, fast and slow subsurface flow components (Figure 5). The model combines a spatially explicit geomorphological unit hydrograph for routing direct runoff and soil-water discharge with a spatially lumped reservoir-based modeling framework for representing delayed storage release from snow and subsurface compartments. This approach provides a parsimonious representation of streamflow generation processes into a set of equations whose key parameters can be calibrated with available data.

The model simulates direct flow (Q_d) from the shallow soil layer using a constant runoff production function (P). The runoff production function (splitting incoming rainfall, R, into direct flow and infiltration into the soil) is parameterized based on the initial abstraction concept of the curve-number approach (Boughton, 1989), where direct flow response to rainfall follows an affine behavior: no response if cumulative rainfall is below a given threshold called initial abstraction (I_a), followed by a linear response:

$$\begin{matrix} R_{eff}(t) = 0 \text{ if } \int_{t_0}^{t} R(t)dt < I_{\mathrm{a}} \\ R_{eff}\big(R(t)\big) = R(t) \text{ otherwise} \end{matrix}, \quad \text{and} \tag{1}$$

$$Q_{\mathrm{d}}(t) = \beta R_{eff}(t), \tag{2}$$

where t_0 is the start of the rain event, and b is the runoff production coefficient (Boughton, 1989). The fraction of rainfall that is not lost to initial abstraction (I_a) or to direct runoff (Q_d) infiltrates into a small soil storage. Discharge from the soil storage (Q_{soil}) is parameterized as a linear function of its storage potential (S_{soil}):

$$Q_{soil}(t) = k_{soil} S_{soil}(t). \tag{3}$$

The volume of soil storage varies between zero and a maximum theoretical storage of $S_{max,soil}$, with excess soil-water drainage infiltrating into the subsurface storages ($I_{subsurface}$):

$$\frac{dS_{soil}(t)}{dt} = \mathrm{R}_{eff}(t) - Q_d(t) - Q_{soil}(t) - I_{subsurface}(t). \tag{4}$$

$$I_{subsurface}(t) = \max(0, S_{soil}(t-1) + \mathrm{R}_{eff}(t) - Q_d(t) - S_{max,soil}). \tag{5}$$

Both Q_d and Q_{soil} represent rainfall directly recharging the stream and are convolved using a geomorphological travel time distribution approach (Rinaldo et al., 1991). The travel time function is split into hillslope and in-stream travel times, with the catchment distributed into 25 sub-catchments (cf. Figure S69 in Michelon, 2022). The hillslope travel time distribution is parameterized by summarizing all topographical flow distances d_H from barycenter of all the

https://doi.org/10.5194/egusphere-2026-4249
Preprint. Discussion started: 17 August 2026

subcatchments (denoted by subscript i in Eq. 6 and 7) to their nearest drainage point in the stream (obtained from catchment geometry) and a constant hillslope velocity (v_H). In-stream travel time is parameterized with a constant stream velocity (v_S) and stream geometry (i.e. distance d_S of each channel head to stream outlet). Catchment and stream geometry parameters were derived from a 2 x 2 m DEM of Vallon de Nant (SwissALTI3D, 2012). The convolution of the rainfall field with the travel-time distribution is implemented as follows:

$$Q_{\mathrm{d}}(t) = \sum_{\mathrm{i} \in \mathrm{catchment}} Q_{d,i}(t) * (\frac{d_{H,i}}{v_{H,i}} + \frac{d_{S,i}}{v_{S,i}})). \quad (6)$$

$$Q_{\mathrm{soil}}(t) = \sum_{\mathrm{i} \in \mathrm{catchment}} Q_{soil,i}(t) * (\frac{d_{H,i}}{v_{H,i}} + \frac{d_{S,i}}{v_{S,i}})). \quad (7)$$

Subsurface flow is divided into two storages (fast and slow). The flow generated from the fast storage (Q_f) is modeled as a nonlinear function of storage volume (S_f), whereas flow from the slow storage (Q_s) is modeled as a linear function of storage volume (S_s) (Roques et al., 2017; Tashie et al., 2020):

$$Q_{\mathrm{f}}(t) = k_{\mathrm{f}} S_{\mathrm{f}}^{\gamma \mathrm{f}}(t), \quad (8)$$

$$Q_{\mathrm{s}}(t) = k_{\mathrm{s}} S_{\mathrm{s}}(t), \quad (9)$$

where k_f, k_s are recession coefficients of the two subsurface storages and γ_f is the exponent of the fast subsurface storage. The fast subsurface storage (S_f) is fed by infiltration of the soil water excess $I_{subsurface}$ (Eq. 10) and the slow subsurface storage (S_s) is fed from the fast subsurface storage (S_f) with a constant flux (L_{max}) limited by the water availability in S_f (Eq. 11) (Schaefli et al., 2014). Both fast and slow subsurface storages are lumped in space and assumed to be fully mixed. The nonlinear storage discharge relationship for fast subsurface flow was essential for simulating fast runoff dynamics and resulted in improved model performance over a linear storage-discharge relationship (Figures S1, S2).

$$\frac{dS_f(t)}{dt} = I_{subsurface}(t) - Q_f(t) - \min\{I_{subsurface}(t), L_{\max}\}. \quad (10)$$

$$\frac{dS_s(t)}{dt} = \min\{I_{subsurface}(t), L_{\max}\} - Q_s(t). \quad (11)$$

Snowmelt originates from a nonlinear storage representing a snowpack:

$$Q_{snow}(t) = k_{snow} S_{snow}^{\gamma snow}(t), \quad (12)$$

where $S_{snow}(t=t_{ini})$, k_{snow}, and γ_{snow} are calibrated together with the other model parameters. The full model is summarized in Figure 5.

https://doi.org/10.5194/egusphere-2026-4249
Preprint. Discussion started: 17 August 2026

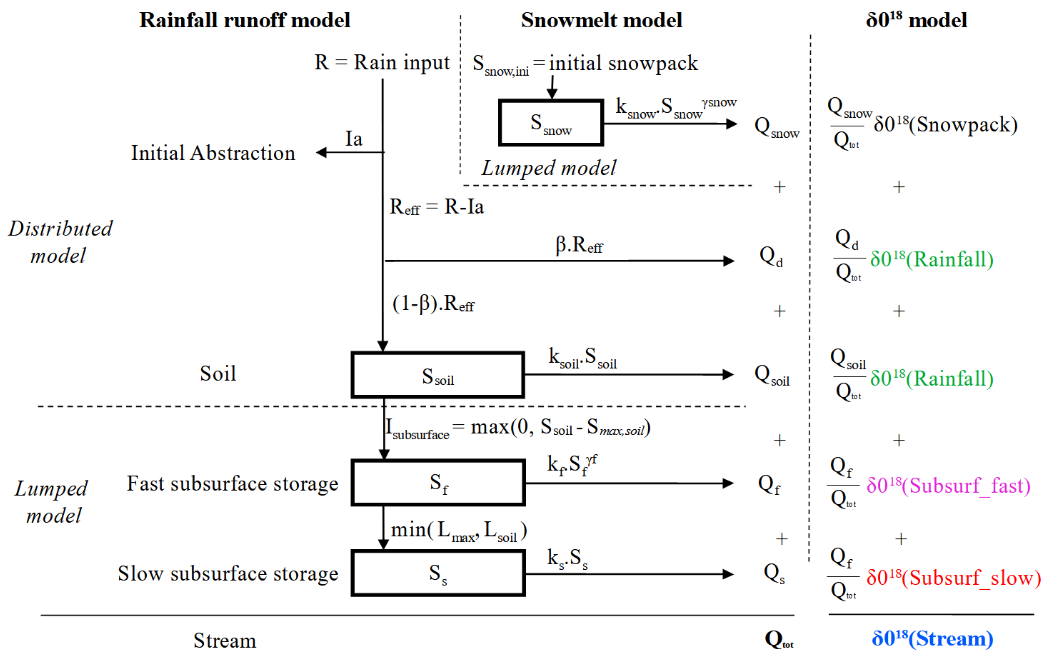

Figure 5: Conceptual representation of the model structure. The soil module is spatially distributed, whereas the snowpack, fast subsurface, and slow subsurface storages are spatially lumped. Each compartment generates discharge as a linear or nonlinear function of storage volume and is assigned an isotopic ratio based on field measurements. Total streamflow is computed as the sum of discharge contributions from different compartments.

4.2 Isotope integration into the model

The partitioning of water fluxes within the catchment is conceptualized as follows. Snowmelt (Q_{snow}) isotopic ratio is assumed to be the average of all snow isotope samples from the preceding winter (distinct values for 2017 and 2018). We acknowledge that using snowpack isotopes instead of snowmelt isotopes might bias the snow end-member as the weighted-average snowmelt isotopic ratios can be higher than snowpack isotopes (Ditlevsen et al., 2025; Noor et al., 2023b, a). We assume this has a relatively small impact on streamflow simulations as the model was run only for the July-September period.

Direct runoff and water leaking out of the soil storage are assumed to originate from rainfall. The isotopic signatures of Q_d and Q_{soil} are therefore set as the average of all rainfall water isotopes from the respective summer season (distinct values for 2017 and 2018). The water released from the two subsurface storages is a mixture of rainfall, snowmelt, and groundwater in unknown proportions. To avoid making assumptions about mixing occurring in subsurface storages, we directly assign Q_{fast} and Q_{slow} isotopes from field observations. The exhaustive spring isotope sampling allowed us to represent the isotopic values of the two subsurface storages.

The isotopic ratio of Q_{fast} is assumed as the average of isotope samples from the three springs that showed fast isotopic and water-temperature dynamics thereby representing faster subsurface flow paths. Q_{slow} isotopic signature is set as

https://doi.org/10.5194/egusphere-2026-4249
Preprint. Discussion started: 17 August 2026

the average of isotope ratios from the remaining two springs which showed slower isotopic and water-temperature dynamics, reflecting slower subsurface flow paths. The isotopic signatures of all five springs vary in time and are represented by frequent field observation. Before averaging, the spring isotope measurements were interpolated in time using thin plate spline.

4.3 Model calibration

To represent the very fast catchment response to summer rainfall events, the model was setup at a 10-minute temporal resolution, forced with high-resolution rainfall data, and calibrated against streamflow and streamwater isotopes aggregated over 10-minute intervals. The model was calibrated within a Bayesian sampling framework, where a Metropolis sampler is used to infer the posterior distribution of the model parameters (Kuczera and Parent, 1998). A Metropolis sampler generates a sequence (or chain) of samples (or parameter sets) from a proposal distribution and accepts each new sample if it has a higher likelihood than the previous sample. If the likelihood is smaller, it still has a chance to be retained. This probabilistic step ensures full sampling of the parameter space. An initial warm-up period to reach steady state was set to 20000 iterations. The posterior parameter distributions were obtained by retaining every 1000th sample of a chain to avoid correlation within successive samples.

A key part of the Metropolis sampler is the evaluation of the likelihood of each proposed parameter set, which is then accepted or rejected depending on if it is better or worse than the likelihood of the previous sample in the chain. Here, we use four distinct likelihood functions defined to account for differences in observations and modeling errors; a new parameter is added to the chain if it passes the likelihood test for each of the four likelihoods. The likelihood function of simulated variable (e.g., for streamflow Q) is specified based on model residuals ε:

$$\varepsilon(t) = Q_{\mathrm{obs}}(t) - Q_{\mathrm{sim}}(t), \quad (13)$$

where model residuals are assumed independent and identically distributed following Gaussian distribution with zero mean and standard deviation σ_e. The log-likelihood (L_s) reads as:

$$L_s = -\frac{n}{2}\log(2\pi\,\sigma_\varepsilon{}^2) - \frac{1}{2\,\sigma_\Delta{}^2}\sum_{i=1}^{n}\varepsilon^2. \quad (14)$$

The four observation datasets involved in the Metropolis algorithm are the following:

- Streamflow observations during low-flow periods, with associated standard deviation σ_e=0.18 mm/h
- Streamflow observations during high-flow periods, with associated standard deviation σ_e=0.36 mm/h
- Streamwater $\delta^{18}O$ isotopic signature during low-flow periods, with associated standard deviation σ_e=0.4‰
- Streamwater $\delta^{18}O$ isotopic signature during high-flow periods, with associated standard deviation σ_e=0.8‰

Different uncertainty levels (shown by σ_e) were assigned to high- and low-flow periods because streamflow intensity and stream isotopic composition strongly fluctuate during high flow conditions, and a small error in the timing of the model simulation is likely to add significant error. Here, high-flow and low-flow periods were delineated visually with high-flow corresponding to the short periods of intense streamflow with sharp temporal fluctuations.

The initial state of the different storages (i.e., S_{snow}, S_{soil}, S_{fast} and S_{slow}) are unknown at the beginning of the summer season and were therefore calibrated first by running the Metropolis algorithm using data from both summer seasons 2017 and 2018, considering that the initial storages and model parameters as unknown. The initial storages were then set to the mean value of the inferred posterior distributions and held fixed for the rest of the calibration procedure. A

https://doi.org/10.5194/egusphere-2026-4249
Preprint. Discussion started: 17 August 2026

split sampling calibration strategy was used for the remaining model parameters, where the model is first calibrated using data for the year 2017 and then evaluated against 2018 data and vice versa. Multiple model diagnostics summarized in Table 1 were used to assess streamflow and streamwater $\delta^{18}O$ simulations.

Table 1: Summary of different statistical indices used to validate the hydrological model (X: observed streamflow; Y: simulated streamflow; n: Number of data points)

Index	Formula	Best value	Worst value
Percentage bias (Pbias)	$\frac{\sum_{i=1}^{n}(X_i - Y_i)}{\sum_{i=1}^{n} X_i} * 100$	0	+∞ / - ∞
Nash Sutcliffe efficiency (NSE)	$1 - \frac{\sum_{i=1}^{n}(X_i - Y_i)^2}{\sum_{i=1}^{n}(X_i - \bar{X})^2}$	1	- ∞ (negative value means that mean is a better estimator than the model).
Root mean squared error (RMSE)	$\sqrt{\frac{\sum_{i=1}^{n}(X_i - Y_i)^2}{n}}$	0	+∞

5. Results

5.1 Streamflow simulations based on discharge and isotope calibrations

Figure 6 compares observed and simulated streamflow during the validation periods for the split-sample calibration strategy. With discharge-only calibration, the model reproduced streamflow dynamics reasonably well, with Nash Sutcliffe efficiencies (NSE) of 0.65 and 0.83 and percentage bias within ±12% for 2017 and 2018, respectively. In 2017 and 2018, most streamflow peaks were captured reasonably well with a few exceptions in the beginning of August for both years, where peak flows were overestimated. Streamflow simulations showed better transferability from the wetter 2017 calibration period to the drier 2018 validation period (Figure 6c,d) than from the drier 2018 calibration period to the wetter 2017 validation period (Figure 6a,b). This suggests that parameter sets inferred from short calibration periods may not transfer well across contrasting hydroclimatic regimes, particularly when the calibration period does not include the full range of rainfall-streamflow dynamics.

Joint calibration with discharge and streamwater isotopes significantly improved streamflow simulations in 2017, as indicated by higher NSE, lower bias and reduced RMSE. Interestingly, streamflow simulations during recession periods following peak flows in 2017 improved significantly (Figure 6b), with joint calibration reducing overestimation in simulated flow. For the 2018 validation period, the streamflow metrics remained broadly similar between discharge-only vs joint calibration. For the large rainfall-streamflow event in beginning of August 2018, joint calibration reduced overestimation of peak flow. This improvement suggests that isotope information might better constrain the partitioning between direct event-water flood generation vs release from subsurface storages, reducing some of the parameter compensation that may occur under discharge-only calibration.

https://doi.org/10.5194/egusphere-2026-4249
Preprint. Discussion started: 17 August 2026

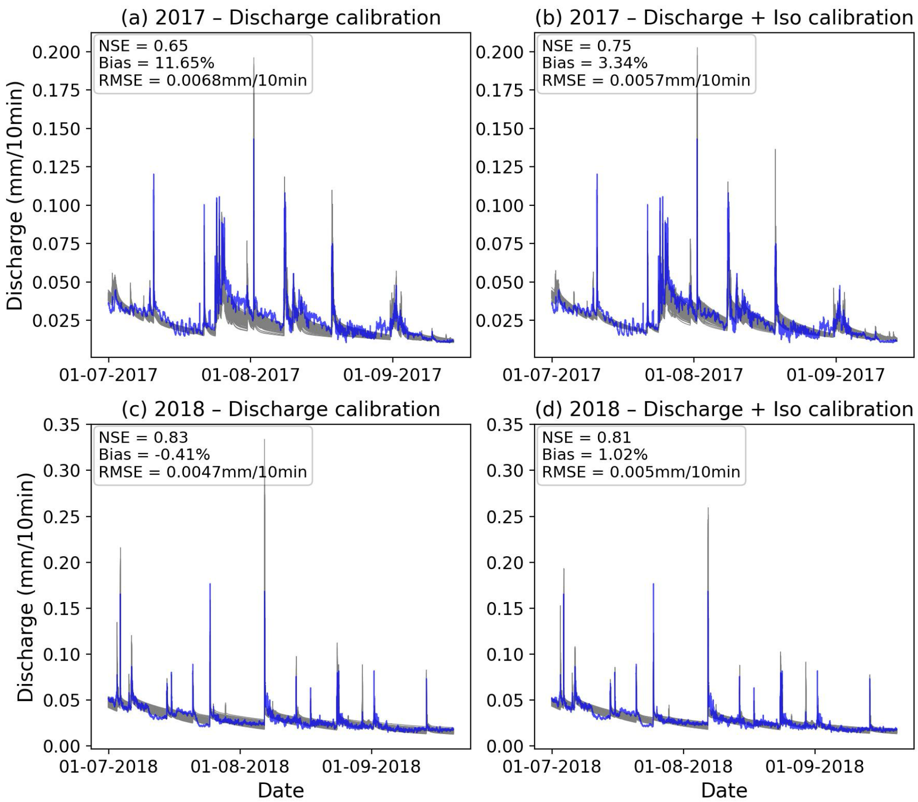

Figure 6: Observed (blue) and simulated (gray) streamflow during the validation periods for the two calibration strategies. Panels a-b show simulations for 2017 using parameters calibrated on 2018 data: (a) discharge-only calibration and (b) joint calibration using discharge and streamwater isotopes. Panels c-d show simulations for 2018 using parameters calibrated on 2017 data: (c) discharge-only calibration and (d) joint calibration using discharge and streamwater isotopes. Streamflow simulations and observations are shown at 10-minute resolution.

5.2 Streamwater isotope simulations based on discharge and isotope calibrations

With discharge-only calibration, the model reproduced the streamwater isotope dynamics reasonably well, especially in 2018 and particularly during high-flow events, when streamwater $\delta^{18}O$ shifted rapidly toward rainfall-like values before returning toward groundwater-like signatures (Figure 7). In 2017 where NSE values for streamwater isotope simulations were negative, the posterior streamwater $\delta^{18}O$ spread still included most of the observed streamwater isotope samples, despite streamwater isotopes not being used in the calibration (Figure 7a). The uncertainty band of simulated streamwater $\delta^{18}O$ remained very large, indicating inadequate constraints in the underlying flow partitioning. Joint calibration with streamflow and streamwater isotopes improved the simulation of streamwater $\delta^{18}O$ in both validation years (Figure 7). For 2017, the improvement was more substantial, with NSE of streamwater $\delta^{18}O$ increasing from -0.07 under discharge-only calibration to 0.49 under joint calibration. The overall isotope dynamics were better reproduced under joint calibration indicating that isotope information better constrain the relative contributions of

https://doi.org/10.5194/egusphere-2026-4249
Preprint. Discussion started: 17 August 2026

rainfall, snowmelt, and subsurface storage during both rainfall and baseflow periods. For 2018, improvement in streamwater δ¹⁸O diagnostics were more modest, with NSE of streamwater δ¹⁸O increasing from 0.62 to 0.67 and RMSE decreasing from 0.35‰ to 0.33‰.

The most noticeable effect of joint calibration is the reduction in predictive uncertainty (Figure 7). In both validation periods, the uncertainty bands around simulated streamwater δ¹⁸O became narrower when isotope data were included in the calibration. This indicates that streamwater isotopes provide additional constraints on parameter combinations that may otherwise produce similar discharge simulations.

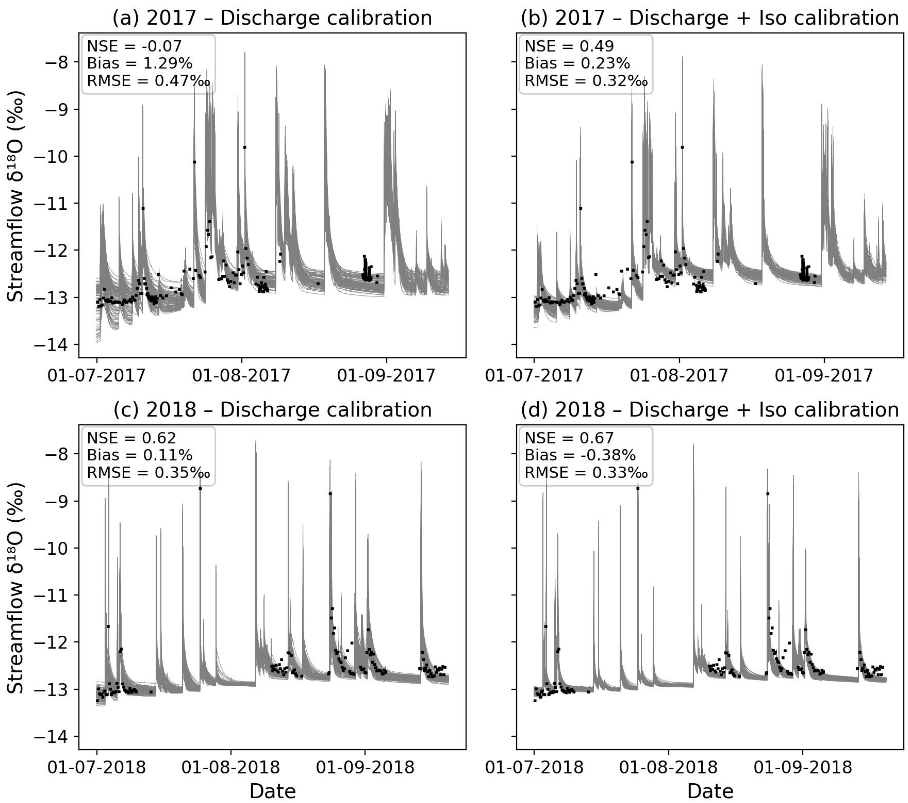

Figure 7: Observed (black dots) and simulated (gray bands) streamwater δ¹⁸O during the validation periods for the two calibration strategies. Panels a-b show simulations for 2017 using parameters calibrated on 2018 data: (a) discharge-only calibration and (b) joint calibration using discharge and streamwater isotopes. Panels c-d show simulations for 2018 using parameters calibrated on 2017 data: (c) discharge-only calibration and (d) joint calibration using discharge and streamwater isotopes. Streamwater isotope simulations are carried out at 10-minute resolution and compared with isotope observations at the time of sample collection.

https://doi.org/10.5194/egusphere-2026-4249
Preprint. Discussion started: 17 August 2026

5.3 Flow partitioning into different components

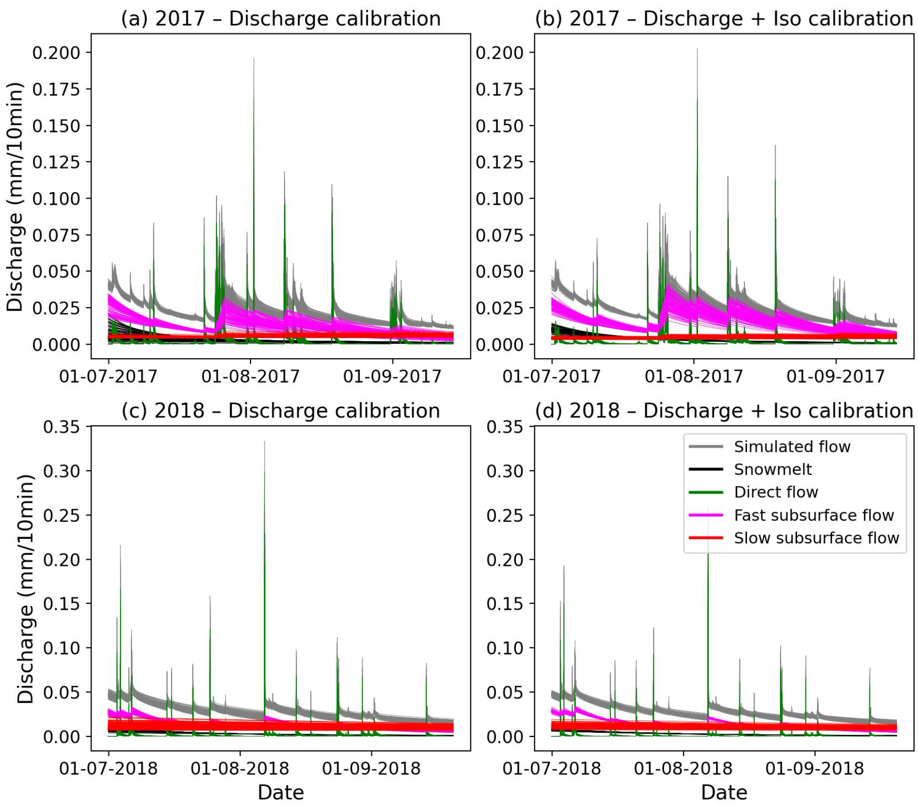

Figure 8: Partitioning of simulated streamflow into snowmelt, direct runoff, fast subsurface flow, and slow subsurface flow for the two calibration strategies. Panels a-b show simulations for 2017 using parameters calibrated on 2018 data: (a) discharge-only calibration and (b) joint calibration using discharge and streamwater isotopes. Panels c-d show simulations for 2018 using parameters calibrated on 2017 data: (c) discharge-only calibration and (d) joint calibration using discharge and streamwater isotopes. Streamflow simulations are carried out at 10-minute resolution.

Figure 8 shows the partitioning of streamflow into snowmelt, direct runoff, fast subsurface flow, and slow subsurface flow for both calibration strategies. Across both summers, direct runoff and snowmelt represented the smallest contributions to total streamflow, whereas subsurface flow dominated streamflow generation (Figure 9). In 2017, streamflow was mainly generated by the fast subsurface component, while in 2018 the contributions from fast and slow subsurface flow were more balanced. This pattern is consistent for both discharge-only and joint discharge-isotope calibration.

This result is particularly important given the very rapid hydrological response of the catchment (Figure 1b). Our simulations showed that this flashy response does not imply high contributions from event-water (direct flow or soil-water discharge). Instead, rainfall rapidly mobilizes water stored in subsurface reservoirs. This supports the

https://doi.org/10.5194/egusphere-2026-4249
Preprint. Discussion started: 17 August 2026

interpretation that rapid streamflow responses in Vallon de Nant are primarily driven by the activation of connected subsurface flow pathways.

Joint calibration with discharge and streamwater isotopes reduced the uncertainty in the simulated flow components (Figure 8), indicating better constrained internal flux partitioning. This effect was most apparent for the subsurface components, but also for snowmelt during early July. In 2017, joint calibration slightly increased the inferred snowmelt contribution during the first two weeks of July, coinciding with diel fluctuations in streamflow (Figure 4) confirming residual snowmelt from high-elevation snow patches. Discharge-only calibration could not constrain snowmelt contribution as clearly (despite the initial snowpack storage being set to the same value in both calibration schemes) and produced larger uncertainty in snowmelt contributions than under joint calibration strategy (compare black lines in Figure 8b vs Figure 8a). Additionally, direct-flow contribution was lower and groundwater contribution was higher under the joint calibration strategy compared to discharge-only calibration (Figure 9).

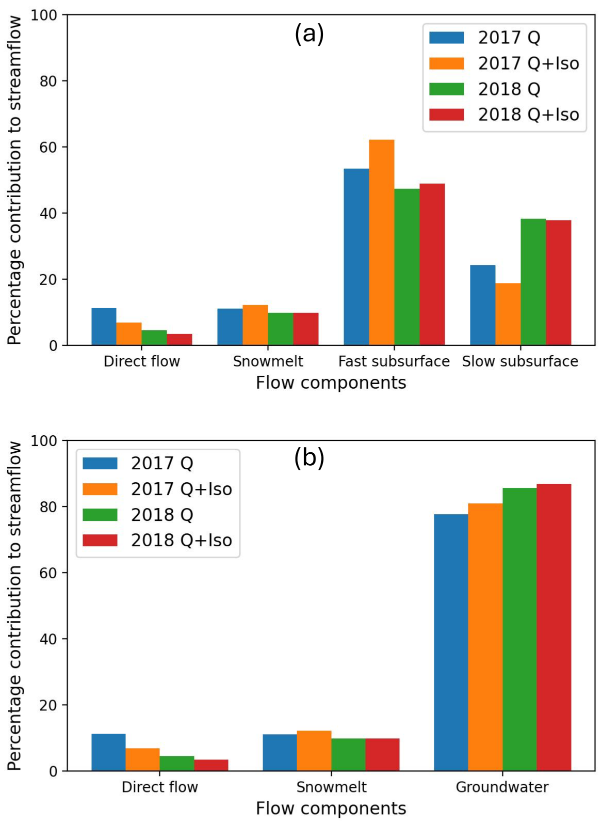

Figure 9: (a) Relative contribution of direct flow, snowmelt, fast subsurface flow, and slow subsurface flow to simulated summer streamflow in 2017 and 2018 for discharge-only calibration and joint calibration using discharge and streamwater isotopes. Panel (b) groups the fast and slow subsurface flows as groundwater flow to contrast event-water contributions with subsurface storage release.

https://doi.org/10.5194/egusphere-2026-4249
Preprint. Discussion started: 17 August 2026

6. **Discussion**

6.1 Groundwater-mediated nonlinear streamflow generation processes

One key result of this study is that fast and slow subsurface flow pathways regulate rapid rainfall-streamflow responses in Vallon de Nant, accounting for more than 80% of simulated summer flow, with smaller contributions from residual snowmelt on steep slopes and direct runoff (Figure 9). Rainfall-derived event water becomes important mainly near peak flow during the most intense rainfall events (Figure 8), and these high event-water contributions persist only for a few hours. This interpretation is consistent with a long history of isotope-based hydrograph separation and modeling studies showing that stormflow is often dominated by pre-event water (Avesani et al., 2025; Dewalle et al., 1988; von Freyberg et al., 2018; Frisbee et al., 2011; Nan and Tian, 2024; Weiler et al., 2003). Our results extend this body of evidence to a snow-influenced, high-relief Swiss alpine catchment with rapid rainfall-streamflow response.

In the model, groundwater-mediated streamflow is generated using two subsurface storages, one with a nonlinear and the other with a linear storage-discharge relationship. This model structure reproduces the rapid streamflow increases during summer storms while maintaining the strong dampening in streamwater isotopes during baseflow conditions and enrichment in stream isotopes during rainfall events. This suggests that rainfall activates subsurface flow pathways and mobilizes previously stored water rather than directly transmitting event water to the stream via preferential flow pathways or overland flow. Such an interpretation is consistent with increased hydrological connectivity during rainfall events, when rising hydraulic gradients near the stream network rapidly mobilize well-mixed shallow groundwater (Sklash et al., 1976). A similar two-reservoir structure was used by Weiler et al., (2003) to represent both streamflow and its isotope dynamics in the Maimai catchment, although streamflow originating from their reservoirs only used linear storage-discharge relationship. In Vallon de Nant, tests using only linear subsurface storage-discharge relationship produced poorer streamflow simulations (Figure S1).

The importance of nonlinear subsurface release is consistent with recent isotope-enabled modeling in mountain environments. For example, Li et al., (2025) used a nonlinear storage-discharge formulation in a glacierized Tibetan Plateau catchment and reported that 60-65% of streamflow originated from shallow and deep subsurface flow pathways. The larger groundwater contribution of up to 80% inferred in Vallon de Nant may reflect its wetter hydroclimatic setting, with annual precipitation of ~1900 mm compared with ~450 mm in the catchment studied by Li et al., (2025). Higher groundwater contributions are expected in wetter landscapes with larger antecedent storage, consistent with von Freyberg et al., (2018), who showed that pre-event water contributions depend strongly on antecedent moisture conditions.

However, the inferred fast and slow groundwater components should be interpreted as a conceptual depiction of effective flow pathways, because our model does not resolve three-dimensional groundwater flow, subsurface topography, or storage in quaternary deposits, which may be important in alpine landscapes (Gentile et al., 2023). Testing whether the inferred fast subsurface flow corresponds to physically identifiable subsurface flow structures would require additional work combining isotope observations with geophysical information and physically-based groundwater modeling.

https://doi.org/10.5194/egusphere-2026-4249
Preprint. Discussion started: 17 August 2026

6.2 Added value of high-resolution isotope-constrained calibration on flow partitioning

Streamwater isotopes provide additional constraints on internal flow partitioning, as shown by the reduced uncertainty in the simulated streamwater $\delta^{18}O$ and partitioning among distinct flow components (Figures 7 and 8). One clear benefit of isotope calibration is the improved representation of residual snowmelt in early summer 2017. Streamflow displayed diel fluctuations in early July 2017 (Figure 4), suggesting snowmelt influences from high-elevation snow patches, but discharge-only calibration could not constrain the magnitude of this contribution (Figure 7a). Because snowmelt is isotopically depleted relative to summer rainfall and groundwater, streamwater $\delta^{18}O$ provides an additional constraint on snow-derived water. Joint streamflow and isotope calibration therefore better constrained the inferred snowmelt contribution during early July 2017 (Figures 8b, 9). This supports previous work showing that isotopes can constrain meltwater contributions in snow- and glacier-influenced catchments (He et al., 2019; Müller et al., 2025; Yong et al., 2026). The improved flow partitioning is also consistent with previous modeling studies showing that isotope data can improve parameter identifiability and constrain internal flow pathways, storage dynamics, and streamflow sources (Avesani et al., 2025; He et al., 2019; Holmes et al., 2023; Nan and Tian, 2024; Stadnyk et al., 2013; Stadnyk and Holmes, 2020, 2023). Isotope calibration therefore reduces the risk of obtaining the right streamflow simulation for the wrong reasons (Beven and Freer, 2001; Kirchner, 2006).

At the same time, joint calibration may not improve all discharge-related metrics. In Vallon de Nant, isotope-informed calibration improved aggregate streamflow simulations in 2017, but not in 2018 when discharge-only calibration already produced reasonable streamflow simulations (Figure 6). Similar results have been reported in other isotope-enabled modeling studies, where streamwater isotope calibration improve the realism of internal flux partitioning while sometimes reducing the accuracy of streamflow performance (Holmes et al., 2020; Jung et al., 2025; Müller et al., 2025). In our case, incorporating stream isotope ratios in calibration did not worsen streamflow simulations.

The 10-minute temporal resolution of this study is particularly important for interpreting rapid mobilization of water during summer storms. Streamwater $\delta^{18}O$ responded rapidly during these rainfall events, shifting toward rainfall-like values during peak flows and returning toward groundwater-like values within 6 to 24 hours (Figure 4). These short-lived isotope dynamics, also seen in other landscapes (Binet et al., 2026), would be missed by lower frequency isotope sampling. As high-frequency sub-daily isotope measurements become more widely available (von Freyberg et al., 2017), comparisons across catchments will refine how rapid subsurface mobilization can be represented in isotope-enabled hydrological models.

6.3 Interannual variability and implications for alpine groundwater storage

The model simulations indicate a clear interannual contrast between fast and slow subsurface flow contributions between the wetter summer of 2017 (encompassing some long-lasting rainfall events) and the drier summer of 2018. In 2017, the fast subsurface component contributed more prominently to streamflow, consistent with observed wetter summer conditions and expected stronger hydrological connectivity. In 2018, the slow subsurface component became relatively more important, suggesting greater reliance on deeper and less responsive groundwater flow pathways during drier summer conditions. This may also reflect greater recharge of slow subsurface storage during the preceding

https://doi.org/10.5194/egusphere-2026-4249
Preprint. Discussion started: 17 August 2026

2017-18 winter and spring, when higher snow accumulation and rapid melt enhanced recharge of the slow subsurface store (Michelon, 2022).

These results suggest that summer streamflow in alpine headwaters during dry years may become increasingly dependent on deeper groundwater storage that are primarily recharged by snowmelt. This interpretation is consistent with recent work highlighting the role of mountain groundwater in sustaining streamflow under changing precipitation and snow regimes (Carroll et al., 2019; van Tiel et al., 2024), and with modeling evidence that drier years can further increase reliance on older groundwater (Siirila-Woodburn et al., 2026). If future summer conditions become drier, as projected in recent climate assessments for Switzerland (MeteoSwiss and Zurich, 2025), slow subsurface storage may become increasingly important for sustaining summer low flows, assuming snowmelt or rainfall-related spring recharge remains significant. Testing this hypothesis will require additional years with contrasting snow and rainfall conditions, ideally combined with high-frequency isotope observations and distributed snow measurements.

7. Limitations

Several limitations should be considered when interpreting the inferred flow partitioning. First, the rainfall-streamflow simulations were restricted to the July-September periods of 2017 and 2018, when high-resolution rainfall fields from the Pluvimate network and sub-daily streamwater isotope observations were available. Although this period is shorter than a full hydrological year, it was well suited for analyzing rapid rainfall-streamflow responses during mostly convective summer storms in Vallon de Nant, as winter and spring precipitation are primarily stratiform (Benoit et al., 2018, 2024). Extending the simulations to full year would require a more detailed representation of snow dynamics, ideally constrained by snow depth or snow water equivalent observations across the spatial gradient. Maintaining sub-daily stream and snow isotope sampling during winter is very challenging in Vallon de Nant because snow accumulation and avalanches limit catchment access.

Second, evapotranspiration is not explicitly represented in the current model structure, and its effects were most likely included in the initial abstraction component of the model. This simplification was deemed acceptable as the main objective of this study is to understand short-timescale streamflow generation processes during high-flow summer periods, but it limits the use of the model for annual water-balance analyses. Canopy-intercepted losses are oversimplified through the runoff-production formulation (Eq. 1). Future applications over longer periods should include a more realistic evapotranspiration component, constrained by distributed meteorological forcings and the spatial distribution of forest and vegetation cover.

Third, the snowmelt representation is deliberately simple. Because the modeling period started in July, most seasonal snow had already disappeared from large parts of the catchment, and snowmelt contributions are expected to be smaller relative to groundwater contributions. The snow model component is mainly intended to represent residual high-elevation snowmelt going rapidly to the stream without recharging subsurface storages, and to reproduce the depleted streamwater isotope signal in early summer (Figure 4). Applying the model to the main melt season would require a more process-based snow module, including elevation-dependent accumulation, wind-driven snow redistribution, radiation-driven snowmelt, recharge of subsurface storages through snowmelt, and possibly rain-on-snow dynamics.

https://doi.org/10.5194/egusphere-2026-4249
Preprint. Discussion started: 17 August 2026

Fourth, the subsurface storages used here are conceptual representations of subsurface rather than direct representations of underlying aquifers. Their isotopic compositions were constrained using spring observations, which provided useful process information but did not fully resolve spatial heterogeneity in subsurface mixing and connectivity. The inferred fast and slow subsurface components should therefore be interpreted as functional flow pathways. Additional years with contrasting snowfall and rainfall conditions would be needed to test the robustness of the inferred subsurface storage-discharge relationships.

Fifth and finally, the error model used in the Metropolis sampler assumes independent and identically distributed model residuals following a Gaussian distribution with a preset standard deviation, neglecting temporal correlation in model residuals. In addition, the current modeling scheme combines effects of model uncertainty and observation errors into a single likelihood function. Future work should implement error models that account for the temporal correlation in model residuals and allow self-calibration of errors' standard deviation (Evin et al., 2013; Schaefli and Kavetski, 2017). Other avenues for improving error model can include characterizing rainfall errors using conditional geostatistical simulation (Renard et al., 2011) and accounting for the variability of the isotopic signature of the different water fluxes using bootstrapping approaches (Beria et al., 2020).

8. Conclusions

We developed a parsimonious model to encode our perceptual model of Vallon de Nant to parameterize streamflow-generation processes in this steep headwater catchment in the Swiss Alps. The model combines a spatially distributed Geomorphological Instantaneous Unit Hydrograph for direct runoff and soil-water drainage (not involving mobilization of water stored in the subsurface) and two lumped subsurface storages representing fast and slow groundwater flow pathways. The model uses high-resolution spatial rainfall measurements and isotope observations in different hydrological fluxes and simulates streamflow and streamwater $\delta^{18}O$ at 10-minute resolution over two consecutive summers. It is not a full water-balance model, the model was run only for the summer periods, and the initial storages were calibrated along with the other model parameters using a Monte Carlo sampling approach.

Despite streamflow peaking approximately 50 minutes after rainfall peaks, our model simulations show that more than 80% of summer streamflow is generated through subsurface flow pathways, while direct runoff and snowmelt account for the remaining contributions. A nonlinear storage-discharge relationship for the fast subsurface reservoir allows modeling the rapid mobilization of shallow groundwater after rainstorms without requiring large direct runoff contributions. Joint calibration with discharge and streamwater isotopes improves streamwater $\delta^{18}O$ simulations, better represents snowmelt contributions, and improves inferred flow partitioning.

Overall, our results show that stable water isotopes provide independent constraints on rapid streamflow-generation processes in a steep alpine catchment, especially when combined with high-resolution rainfall and streamflow observations. The approach highlights the dominant role of groundwater pathways in sustaining both low flows and storm responses during summer periods in Vallon de Nant.

https://doi.org/10.5194/egusphere-2026-4249
Preprint. Discussion started: 17 August 2026

Data availability

Stable water isotope data for the different fluxes used in this paper are available at https://zenodo.org/records/7540709. 10-minute rainfall estimates were aggregated based on 2-minute rainfall timeseries available at https://zenodo.org/records/3946242. Streamflow records are available at https://zenodo.org/records/15739350.

Author contributions

HB and LB formulated and implemented the conceptual underpinnings of the model. LB and GM designed and managed the precipitation observation field campaign. NC designed and managed all other aspects of the field study and laboratory analysis. HB contributed to field and laboratory work. BS acquired the funding for the isotope work. HB, LB, BS, NC and GM interpreted the results and provided critical feedback during model validation. HB conducted the data analysis and wrote the first draft. All authors reviewed, edited and revised the manuscript.

Competing interests

The authors declare that they have no conflict of interest.

Acknowledgements

We credit Anthony Michelon for extensive fieldwork and majority of laboratory analysis of the water samples. We thank James Kirchner for insightful discussions on mechanisms explaining streamflow generation processes in Vallon de Nant.

Financial support

This research has been supported by the Swiss National Science Foundation (grant number: PP00P2_157611). HB acknowledges funding from the CryoSCOPE project (grant number: 101184736), supported by the State Secretariat for Education, Research and Innovation (SERI) under the European Union's Horizon Europe research and innovation program.

References

Akers, P. D., Welker, J. M., and Brook, G. A.: Reassessing the role of temperature in precipitation oxygen isotopes across the eastern and central United States through weekly precipitation-day data, Water Resour. Res., 53, 7644–7661, https://doi.org/10.1002/2017WR020569, 2017.

Avesani, D., Nan, Y., and Tian, F.: Reducing hydrological uncertainty in large mountainous basins: the role of isotope, snow cover, and glacier dynamics in capturing streamflow seasonality, Hydrol. Earth Syst. Sci., 29, 5755–5775, https://doi.org/10.5194/hess-29-5755-2025, 2025.

Bai, P., Liu, X., and Liu, C.: Improving hydrological simulations by incorporating GRACE data for model calibration, J. Hydrol. (Amst)., 557, 291–304, https://doi.org/10.1016/j.jhydrol.2017.12.025, 2018.

Benettin, P., Soulsby, C., Birkel, C., Tetzlaff, D., Botter, G., and Rinaldo, A.: Using SAS functions and high-resolution isotope data to unravel travel time distributions in headwater catchments, Water Resour. Res., 53, 1864–1878, https://doi.org/10.1002/2016WR020117, 2017.

Benoit, L., Allard, D., and Mariethoz, G.: Stochastic Rainfall Modeling at Sub-kilometer Scale, Water Resour. Res., 54, 4108–4130, https://doi.org/10.1029/2018WR022817, 2018.

Benoit, L., Koch, E., Peleg, N., and Mariethoz, G.: Precipitation-elevation relationship: Non-linearity and space–time variability prevail in the Swiss Alps, J. Hydrol. X, 25, 100186, https://doi.org/10.1016/j.hydroa.2024.100186, 2024.

Beria, H., Larsen, J. R., Ceperley, N. C., Michelon, A., Vennemann, T., and Schaefli, B.: Understanding snow hydrological processes through the lens of stable water isotopes, Wiley Interdisciplinary Reviews: Water, 5, e1311, https://doi.org/10.1002/wat2.1311, 2018.

Beria, H., Larsen, J. R., Michelon, A., Ceperley, N. C., and Schaefli, B.: HydroMix v1.0: a new Bayesian mixing framework for attributing uncertain hydrological sources, Geosci. Model Dev., 13, 2433–2450, https://doi.org/10.5194/gmd-13-2433-2020, 2020.

Beven, K. and Freer, J.: Equifinality, data assimilation, and uncertainty estimation in mechanistic modelling of complex environmental systems using the GLUE methodology, J. Hydrol. (Amst)., 249, 11–29, https://doi.org/10.1016/S0022-1694(01)00421-8, 2001.

Binet, S., Rosset, T., Gascoin, S., Le Roux, G., Deschamps-Berger, C., Durántez Jiménez, P., Payre-Suc, V., Granouillac, F., Moussa, I., and Gandois, L.: Water Oxygen Isotope Thermometer in Headwaters: Indicating Groundwater Recharge and Peatland Water Dependence on Air Temperature, Hydrol. Process., 40, e70465, https://doi.org/10.1002/hyp.70465, 2026.

Birkel, C., Duvert, C., Correa, A., Munksgaard, N. C., Maher, D. T., and Hutley, L. B.: Tracer-Aided Modeling in the Low-Relief, Wet-Dry Tropics Suggests Water Ages and DOC Export Are Driven by Seasonal Wetlands and Deep Groundwater, Water Resour. Res., 56, e2019WR026175, https://doi.org/10.1029/2019WR026175, 2020.

Boughton, W. C.: A review of the USDA SCS curve number method, Soil Research, 27, 511–523, 1989.

Brunner, M. I., Sikorska, A. E., and Seibert, J.: Bivariate analysis of floods in climate impact assessments, Science of The Total Environment, 616–617, 1392–1403, https://doi.org/10.1016/j.scitotenv.2017.10.176, 2018.

Carroll, R. W. H., Deems, J. S., Niswonger, R., Schumer, R., and Williams, K. H.: The Importance of Interflow to Groundwater Recharge in a Snowmelt-Dominated Headwater Basin, Geophys. Res. Lett., 46, 5899–5908, https://doi.org/10.1029/2019GL082447, 2019.

Ceperley, N., Michelon, A., Escoffier, N., Mayoraz, G., Boix Canadell, M., Horgby, A., Hammer, F., Antoniazza, G., Schaefli, B., Lane, S., Rickenmann, D., and Boss, S.: Salt gauging and stage-discharge curve, Avançon de Nant, outlet Vallon de Nant catchment, data set accessible at https://zenodo.org/record/1154798#.Wm7pvjQiG1s, https://doi.org/10.5281/zenodo.1154798, 2018.

Ceperley, N., Zuecco, G., Beria, H., Carturan, L., Michelon, A., Penna, D., Larsen, J., and Schaefli, B.: Seasonal snow cover decreases young water fractions in high Alpine catchments, Hydrol. Process., 34, 4794–4813, https://doi.org/10.1002/hyp.13937, 2020.

Dembélé, M., Hrachowitz, M., Savenije, H. H. G., Mariéthoz, G., and Schaefli, B.: Improving the Predictive Skill of a Distributed Hydrological Model by Calibration on Spatial Patterns With Multiple Satellite Data Sets, Water Resour. Res., 56, e2019WR026085, https://doi.org/10.1029/2019WR026085, 2020a.

Dembélé, M., Ceperley, N., Zwart, S. J., Salvadore, E., Mariethoz, G., and Schaefli, B.: Potential of satellite and reanalysis evaporation datasets for hydrological modelling under various model calibration strategies, Adv. Water Resour., 143, 103667, https://doi.org/10.1016/j.advwatres.2020.103667, 2020b.

Dewalle, D. R., Swistock, B. R., and Sharpe, W. E.: Three-component tracer model for stormflow on a small Appalachian forested catchment, J. Hydrol. (Amst)., 104, 301–310, https://doi.org/10.1016/0022-1694(88)90171-0, 1988.

Ditlevsen, C., Marttila, H., and Ala-aho, P.: Stable Water Isotope Signal of Snow Meltwater: Testing Three Different Measurement Setups in Boreal-Subarctic Conditions, Hydrol. Process., 39, e70277, https://doi.org/10.1002/hyp.70277, 2025.

Eeckman, J., De Grenus, B., Miesen, F. M., Thornton, J., Brunner, P., and Peleg, N.: Multi-instrumental monitoring of snowmelt infiltration in Vallon de Nant, Swiss Alps, Hydrol. Earth Syst. Sci., 29, 4093–4107, https://doi.org/10.5194/hess-29-4093-2025, 2025.

Evin, G., Kavetski, D., Thyer, M., and Kuczera, G.: Pitfalls and improvements in the joint inference of heteroscedasticity and autocorrelation in hydrological model calibration, Water Resour. Res., 49, 4518–4524, https://doi.org/10.1002/wrcr.20284, 2013.

von Freyberg, J., Studer, B., and Kirchner, J. W.: A lab in the field: high-frequency analysis of water quality and stable isotopes in stream water and precipitation, Hydrol. Earth Syst. Sci., 21, 1721–1739, https://doi.org/10.5194/hess-21-1721-2017, 2017.

von Freyberg, J., Studer, B., Rinderer, M., and Kirchner, J. W.: Studying catchment storm response using event- and pre-event-water volumes as fractions of precipitation rather than discharge, Hydrol. Earth Syst. Sci., 22, 5847–5865, https://doi.org/10.5194/hess-22-5847-2018, 2018.

Friedman, I., Redfield, A. C., Schoen, B., and Harris, J.: The variation of the deuterium content of natural waters in the hydrologic cycle, Reviews of Geophysics, 2, 177–224, https://doi.org/10.1029/RG002i001p00177, 1964.
Frisbee, M. D., Phillips, F. M., Campbell, A. R., Liu, F., and Sanchez, S. A.: Streamflow generation in a large, alpine watershed in the southern Rocky Mountains of Colorado: Is streamflow generation simply the aggregation of hillslope runoff responses?, Water Resour. Res., 47, https://doi.org/10.1029/2010WR009391, 2011.
Gentile, A., Canone, D., Ceperley, N., Gisolo, D., Previati, M., Zuecco, G., Schaefli, B., and Ferraris, S.: Towards a conceptualization of the hydrological processes behind changes of young water fraction with elevation: a focus on mountainous alpine catchments, Hydrol. Earth Syst. Sci., 27, 2301–2323, https://doi.org/10.5194/hess-27-2301-2023, 2023.
Harman, C. J.: Age-Ranked Storage-Discharge Relations: A Unified Description of Spatially Lumped Flow and Water Age in Hydrologic Systems, Water Resour. Res., 55, 7143–7165, https://doi.org/10.1029/2017WR022304, 2019.
He, Z., Unger-Shayesteh, K., Vorogushyn, S., Weise, S. M., Kalashnikova, O., Gafurov, A., Duethmann, D., Barandun, M., and Merz, B.: Constraining hydrological model parameters using water isotopic compositions in a glacierized basin, Central Asia, J. Hydrol. (Amst)., 571, 332–348, https://doi.org/10.1016/j.jhydrol.2019.01.048, 2019.
Holmes, T., Stadnyk, T. A., Kim, S. J., and Asadzadeh, M.: Regional Calibration With Isotope Tracers Using a Spatially Distributed Model: A Comparison of Methods, Water Resour. Res., 56, e2020WR027447, https://doi.org/10.1029/2020WR027447, 2020.
Holmes, T. L., Stadnyk, T. A., Asadzadeh, M., and Gibson, J. J.: Guidance on large scale hydrologic model calibration with isotope tracers, J. Hydrol. (Amst)., 621, 129604, https://doi.org/10.1016/J.JHYDROL.2023.129604, 2023.
Hrachowitz, M. and Clark, M. P.: HESS Opinions: The complementary merits of competing modelling philosophies in hydrology, Hydrol. Earth Syst. Sci., 21, 3953–3973, https://doi.org/10.5194/hess-21-3953-2017, 2017.
Hrachowitz, M., Benettin, P., van Breukelen, B. M., Fovet, O., Howden, N. J. K., Ruiz, L., van der Velde, Y., and Wade, A. J.: Transit times—the link between hydrology and water quality at the catchment scale, Wiley Interdisciplinary Reviews: Water, 3, 629–657, https://doi.org/10.1002/wat2.1155, 2016.
van Huijgevoort, M. H. J., Tetzlaff, D., Sutanudjaja, E. H., and Soulsby, C.: Using high resolution tracer data to constrain water storage, flux and age estimates in a spatially distributed rainfall-runoff model, Hydrol. Process., 30, 4761–4778, https://doi.org/10.1002/hyp.10902, 2016.
Jung, H., Tetzlaff, D., Birkel, C., and Soulsby, C.: Recent Developments and Emerging Challenges in Tracer-Aided Modeling, WIREs Water, 12, e70015, https://doi.org/10.1002/wat2.70015, 2025.
Kirchner, J. W.: A double paradox in catchment hydrology and geochemistry, Hydrol. Process., 17, 871–874, https://doi.org/10.1002/hyp.5108, 2003.
Kirchner, J. W.: Getting the right answers for the right reasons: Linking measurements, analyses, and models to advance the science of hydrology, Water Resour. Res., 42, https://doi.org/10.1029/2005WR004362, 2006.
Kirchner, J. W.: Characterizing nonlinear, nonstationary, and heterogeneous hydrologic behavior using ensemble rainfall–runoff analysis (ERRA): proof of concept, Hydrol. Earth Syst. Sci., 28, 4427–4454, https://doi.org/10.5194/hess-28-4427-2024, 2024.
Kirchner, J. W., Benettin, P., and van Meerveld, I.: Instructive Surprises in the Hydrological Functioning of Landscapes, Annu. Rev. Earth Planet. Sci., 51, 277–299, https://doi.org/10.1146/annurev-earth-071822-100356, 2023.
Klaus, J. and McDonnell, J. J.: Hydrograph separation using stable isotopes: Review and evaluation, J. Hydrol. (Amst)., 505, 47–64, https://doi.org/10.1016/j.jhydrol.2013.09.006, 2013.
Knighton, J., Souter-Kline, V., Volkman, T., Troch, P. A., Kim, M., Harman, C., Morris, C., Buchanan, B., and Walter, M. T.: Seasonal and Topographic Variations in Ecohydrological Separation Within a Small, Temperate, Snow-Influenced Catchment, Water Resour. Res., 55, 6417–6435, https://doi.org/10.1029/2019WR025174, 2019.
Knighton, J., Kuppel, S., Smith, A., Soulsby, C., Sprenger, M., and Tetzlaff, D.: Using isotopes to incorporate tree water storage and mixing dynamics into a distributed ecohydrologic modelling framework, Ecohydrology, 13, e2201, https://doi.org/10.1002/eco.2201, 2020.
Kuczera, G. and Parent, E.: Monte Carlo assessment of parameter uncertainty in conceptual catchment models: the Metropolis algorithm, J. Hydrol. (Amst)., 211, 69–85, https://doi.org/10.1016/S0022-1694(98)00198-X, 1998.
Kunnath-Poovakka, A., Ryu, D., Renzullo, L. J., and George, B.: The efficacy of calibrating hydrologic model using remotely sensed evapotranspiration and soil moisture for streamflow prediction, J. Hydrol. (Amst)., 535, 509–524, https://doi.org/10.1016/j.jhydrol.2016.02.018, 2016.

https://doi.org/10.5194/egusphere-2026-4249
Preprint. Discussion started: 17 August 2026

Kuppel, S., Tetzlaff, D., Maneta, M. P., and Soulsby, C.: EcH2O-iso 1.0: water isotopes and age tracking in a process-based, distributed ecohydrological model, Geosci. Model Dev., 11, 3045–3069, https://doi.org/10.5194/gmd-11-3045-2018, 2018.

Li, G., Chen, X., Gao, M., Zhang, Z., Soulsby, C., Tetzlaff, D., and Wang, Y.: Stepwise tracer-based hydrograph separation to quantify contributions of multiple sources of streamflow in a large glacierized catchment over the Tibetan Plateau, J. Hydrol. (Amst)., 662, 134083, https://doi.org/10.1016/j.jhydrol.2025.134083, 2025.

Malhi, Y., Franklin, J., Seddon, N., Solan, M., Turner, M. G., Field, C. B., and Knowlton, N.: Climate change and ecosystems: threats, opportunities and solutions, Philosophical Transactions of the Royal Society B: Biological Sciences, 375, 20190104, https://doi.org/10.1098/rstb.2019.0104, 2020.

Mcdonnell, J. J. and Beven, K.: Debates - The future of hydrological sciences: A (common) path forward? A call to action aimed at understanding velocities, celerities and residence time distributions of the headwater hydrograph, Water Resour. Res., 50, 5342–5350, https://doi.org/10.1002/2013WR015141, 2014.

MeteoSwiss and Zurich, E.: Climate CH2025 - Scientific Report, Zurich, https://doi.org/10.18751/climate/scenarios/ch2025/sr/1.0/, 2025.

Michelon, A.: Hydrologic processes analysis in a high Alpine catchment: the case of the Vallon de Nant, Université de Lausanne, 2022.

Michelon, A., Benoit, L., Beria, H., Ceperley, N., and Schaefli, B.: Benefits from high-density rain gauge observations for hydrological response analysis in a small alpine catchment, Hydrol. Earth Syst. Sci., 25, 2301–2325, https://doi.org/10.5194/hess-25-2301-2021, 2021.

Michelon, A., Ceperley, N., Beria, H., Larsen, J., Vennemann, T., and Schaefli, B.: Hydrodynamics of a high Alpine catchment characterized by four natural tracers, Hydrol. Earth Syst. Sci., 27, 1403–1430, https://doi.org/10.5194/hess-27-1403-2023, 2023.

Müller, T., Fischer, M., Lane, S. N., and Schaefli, B.: Separating snow and ice melt using water stable isotopes and glacio-hydrological modelling: towards improving the application of isotope analyses in highly glacierized catchments, Cryosphere, 19, 423–458, https://doi.org/10.5194/tc-19-423-2025, 2025.

Nan, Y. and Tian, F.: Isotope data-constrained hydrological model improves soil moisture simulation and runoff source apportionment, J. Hydrol. (Amst)., 633, 131006, https://doi.org/10.1016/j.jhydrol.2024.131006, 2024.

Nijzink, R. C., Almeida, S., Pechlivanidis, I. G., Capell, R., Gustafssons, D., Arheimer, B., Parajka, J., Freer, J., Han, D., Wagener, T., Nooijen, R. R. P., Savenije, H. H. G., and Hrachowitz, M.: Constraining Conceptual Hydrological Models With Multiple Information Sources, Water Resour. Res., 54, 8332–8362, https://doi.org/10.1029/2017WR021895, 2018.

Noor, K., Marttila, H., Welker, J. M., Mustonen, K. R., Kløve, B., and Ala-aho, P.: Snow sampling strategy can bias estimation of meltwater fractions in isotope hydrograph separation, J. Hydrol. (Amst)., 627, 130429, https://doi.org/10.1016/J.JHYDROL.2023.130429, 2023a.

Noor, K., Marttila, H., Klöve, B., Welker, J. M., and Ala-aho, P.: The Spatiotemporal Variability of Snowpack and Snowmelt Water 18O and 2H Isotopes in a Subarctic Catchment, Water Resour. Res., 59, e2022WR033101, https://doi.org/https://doi.org/10.1029/2022WR033101, 2023b.

Obradovic, M. M. and Sklash, M. G.: An isotopic and geochemical study of snowmelt runoff in a small arctic watershed, Hydrol. Process., 1, 15–30, https://doi.org/10.1002/hyp.3360010104, 1986.

Odusanya, A. E., Mehdi, B., Schürz, C., Oke, A. O., Awokola, O. S., Awomeso, J. A., Adejuwon, J. O., and Schulz, K.: Multi-site calibration and validation of SWAT with satellite-based evapotranspiration in a data-sparse catchment in southwestern Nigeria, Hydrol. Earth Syst. Sci., 23, 1113–1144, https://doi.org/10.5194/hess-23-1113-2019, 2019.

Parajka, J. and Blöschl, G.: The value of MODIS snow cover data in validating and calibrating conceptual hydrologic models, J. Hydrol. (Amst)., 358, 240–258, https://doi.org/https://doi.org/10.1016/j.jhydrol.2008.06.006, 2008.

Pearce, A. J., Stewart, M. K., and Sklash, M. G.: Storm Runoff Generation in Humid Headwater Catchments: 1. Where Does the Water Come From?, Water Resour. Res., 22, 1263–1272, https://doi.org/10.1029/WR022i008p01263, 1986.

Pepin, N., Bradley, R. S., Diaz, H. F., Baraer, M., Caceres, E. B., Forsythe, N., Fowler, H., Greenwood, G., Hashmi, M. Z., Liu, X. D., Miller, J. R., Ning, L., Ohmura, A., Palazzi, E., Rangwala, I., Schöner, W., Severskiy, I., Shahgedanova, M., Wang, M. B., Williamson, S. N., Yang, D. Q., and Group, M. R. I. E. D. W. W.: Elevation-dependent warming in mountain regions of the world, Nat. Clim. Chang., 5, 424–430, https://doi.org/10.1038/nclimate2563, 2015.

Pepin, N. C., Arnone, E., Gobiet, A., Haslinger, K., Kotlarski, S., Notarnicola, C., Palazzi, E., Seibert, P., Serafin, S., Schöner, W., Terzago, S., Thornton, J. M., Vuille, M., and Adler, C.: Climate Changes and Their Elevational

https://doi.org/10.5194/egusphere-2026-4249
Preprint. Discussion started: 17 August 2026

Patterns in the Mountains of the World, Reviews of Geophysics, 60, e2020RG000730, https://doi.org/10.1029/2020RG000730, 2022.

Peters-Lidard, C. D., Hossain, F., Leung, L. R., McDowell, N., Rodell, M., Tapiador, F. J., Turk, F. J., and Wood, A.: 100 Years of Progress in Hydrology, Meteorological Monographs, 59, 25.1-25.51, https://doi.org/10.1175/AMSMONOGRAPHS-D-18-0019.1, 2019.

Piovano, T. I., Tetzlaff, D., Carey, S. K., Shatilla, N. J., Smith, A., and Soulsby, C.: Spatially distributed tracer-aided runoff modelling and dynamics of storage and water ages in a permafrost-influenced catchment, Hydrol. Earth Syst. Sci., 23, 2507–2523, https://doi.org/10.5194/hess-23-2507-2019, 2019.

Popp, A. L., Beria, H., Sprenger, M., Ala-Aho, P., Coenders-Gerrits, M., Groh, J., Klaus, J., Knapp, J. L. A., Koren, G., Bakiri, I., Xu Fei, E., Gillon, M., Harman, C., Hissler, C., Holmes, T., Jeelani, G., Kalvans, A., Montemagno, A., Zeray Öztürk, E., Žvab Rožič, P., Stadnyk, T., Stumpp, C., Valiente, N., von Freyberg, J., Vreča, P., Zuecco, G., van Meerveld, I., Penna, D., and Kirchner, J. W.: Recent Advances in Tracer-Aided Mixing Modeling of Water in the Critical Zone, Reviews of Geophysics, 63, e2024RG000866, https://doi.org/10.1029/2024RG000866, 2025.

Rajib, A., Evenson, G. R., Golden, H. E., and Lane, C. R.: Hydrologic model predictability improves with spatially explicit calibration using remotely sensed evapotranspiration and biophysical parameters, J. Hydrol. (Amst)., 567, 668–683, https://doi.org/10.1016/j.jhydrol.2018.10.024, 2018.

Renard, B., Kavetski, D., Leblois, E., Thyer, M., Kuczera, G., and Franks, S. W.: Toward a reliable decomposition of predictive uncertainty in hydrological modeling: Characterizing rainfall errors using conditional simulation, Water Resour. Res., 47, https://doi.org/10.1029/2011WR010643, 2011.

Rinaldo, A., Marani, A., and Rigon, R.: Geomorphological dispersion, Water Resour. Res., 27, 513–525, https://doi.org/10.1029/90WR02501, 1991.

Roques, C., Rupp, D. E., and Selker, J. S.: Improved streamflow recession parameter estimation with attention to calculation of − dQ/dt, Adv. Water Resour., 108, 29–43, https://doi.org/10.1016/J.ADVWATRES.2017.07.013, 2017.

Salvatore, M., Leonardo, M., Fortunato, D. S. S., Caterina, S., and Leonardo, M.: Exploiting the use of physical information for the calibration of a lumped hydrological model, Hydrol. Process., 32, 1420–1433, https://doi.org/10.1002/hyp.11501, 2018.

Schaefli, B. and Kavetski, D.: Bayesian spectral likelihood for hydrological parameter inference, Water Resour. Res., 53, 6857–6884, https://doi.org/10.1002/2016WR019465, 2017.

Schaefli, B., Nicótina, L., Imfeld, C., Da Ronco, P., Bertuzzo, E., and Rinaldo, A.: SEHR-ECHO v1.0: a Spatially Explicit Hydrologic Response model for ecohydrologic applications, Geosci. Model Dev., 7, 2733–2746, https://doi.org/10.5194/gmd-7-2733-2014, 2014.

Schumann, A. H.: Thiessen PolygonThiessen polygon BT - Encyclopedia of Hydrology and Lakes, Springer Netherlands, Dordrecht , 648–649, https://doi.org/10.1007/1-4020-4497-6_220, 1998.

Siirila-Woodburn, E. R., Thiros, N., Newcomer, M., Rudisill, W., Dennedy-Frank, P. J., Feldman, D., Sprenger, M., Carroll, Rosemary. W. H., Williams, K. H., and Brodie, E.: Warming and snow loss increase reliance on old groundwater in a Colorado River headwater, Nat. Geosci., 19, 549–555, https://doi.org/10.1038/s41561-026-01945-y, 2026.

Sklash, M. G., Farvolden, R. N., and Fritz, P.: A conceptual model of watershed response to rainfall, developed through the use of oxygen-18 as a natural tracer, Can. J. Earth Sci., 13, 271–283, https://doi.org/10.1139/e76-029, 1976.

Snarski, J. W., Kuppel, S., Caridad, C., and Knighton, J.: Growing Season Precipitation Percolates to Groundwater Past Older Water in Storage Across a Temperate Agricultural Catchment, Water Resour. Res., 61, e2024WR038869, https://doi.org/10.1029/2024WR038869, 2025.

Sodemann, H. and Zubler, E.: Seasonal and inter-annual variability of the moisture sources for Alpine precipitation during 1995–2002, International Journal of Climatology, 30, 947–961, https://doi.org/10.1002/joc.1932, 2010.

Stadnyk, T. A. and Holmes, T. L.: On the value of isotope-enabled hydrological model calibration, Hydrological Sciences Journal, 1–14, https://doi.org/10.1080/02626667.2020.1751847, 2020.

Stadnyk, T. A. and Holmes, T. L.: Large scale hydrologic and tracer aided modelling: A review, J. Hydrol. (Amst)., 618, 129177, https://doi.org/10.1016/J.JHYDROL.2023.129177, 2023.

Stadnyk, T. A., Delavau, C., Kouwen, N., and Edwards, T. W. D.: Towards hydrological model calibration and validation: simulation of stable water isotopes using the isoWATFLOOD model, Hydrol. Process., 27, 3791–3810, https://doi.org/10.1002/hyp.9695, 2013.

Stoffel, M., Wyżga, B., Niedźwiedź, T., Ruiz-Villanueva, V., Ballesteros-Cánovas, J. A., and Kundzewicz, Z. W.: Floods in Mountain Basins BT - Flood Risk in the Upper Vistula Basin, edited by: Kundzewicz, Z. W., Stoffel, M.,

Niedźwiedź, T., and Wyżga, B., Springer International Publishing, Cham, 23–37, https://doi.org/10.1007/978-3-319-41923-7_2, 2016.
Stott, P.: How climate change affects extreme weather events, Science (1979)., 352, 1517–1518, https://doi.org/10.1126/science.aaf7271, 2016.
Sutanudjaja, E. H., van Beek, L. P. H., de Jong, S. M., van Geer, F. C., and Bierkens, M. F. P.: Calibrating a large-extent high-resolution coupled groundwater-land surface model using soil moisture and discharge data, Water Resour. Res., 50, 687–705, https://doi.org/10.1002/2013WR013807, 2014.
SwissALTI3D: The digital elevation model of Switzerland, 2012.
Tashie, A., Pavelsky, T., and Emanuel, R. E.: Spatial and Temporal Patterns in Baseflow Recession in the Continental United States, Water Resour. Res., 56, e2019WR026425, https://doi.org/10.1029/2019WR026425, 2020.
Thornton, J. M., Mariethoz, G., and Brunner, P.: A 3D geological model of a structurally complex Alpine region as a basis for interdisciplinary research, Sci. Data, 5, 180238, https://doi.org/10.1038/sdata.2018.238, 2018.
Thornton, J. M., Therrien, R., Mariéthoz, G., Linde, N., and Brunner, P.: Simulating Fully-Integrated Hydrological Dynamics in Complex Alpine Headwaters: Potential and Challenges, Water Resour. Res., 58, e2020WR029390, https://doi.org/10.1029/2020WR029390, 2022.
van Tiel, M., Aubry-Wake, C., Somers, L., Andermann, C., Avanzi, F., Baraer, M., Chiogna, G., Daigre, C., Das, S., Drenkhan, F., Farinotti, D., Fyffe, C. L., de Graaf, I., Hanus, S., Immerzeel, W., Koch, F., McKenzie, J. M., Müller, T., Popp, A. L., Saidaliyeva, Z., Schaefli, B., Schilling, O. S., Teagai, K., Thornton, J. M., and Yapiyev, V.: Cryosphere–groundwater connectivity is a missing link in the mountain water cycle, Nature Water, 2, 624–637, https://doi.org/10.1038/s44221-024-00277-8, 2024.
Tunaley, C., Tetzlaff, D., Birkel, C., and Soulsby, C.: Using high resolution isotope data and alternative calibration strategies for a tracer-aided runoff model in a nested catchment, Hydrol. Process., 31, 3962–3978, https://doi.org/10.1002/hyp.11313, 2017.
Watson, A., Vystavna, Y., Kralisch, S., Jörg Helmschrot, |, Van Rooyen, J., and Miller, J.: Towards the development of an isotope-enabled rainfall-runoff model: Improving the ability to capture hydrological and anthropogenic change, Hydrol. Process., 37, e14819, https://doi.org/10.1002/HYP.14819, 2023.
Weiler, M., McGlynn, B. L., McGuire, K. J., and McDonnell, J. J.: How does rainfall become runoff? A combined tracer and runoff transfer function approach, Water Resour. Res., 39, n/a-n/a, https://doi.org/10.1029/2003WR002331, 2003.
Weingartner, R., Barben, M., and Spreafico, M.: Floods in mountain areas—an overview based on examples from Switzerland, J. Hydrol. (Amst)., 282, 10–24, https://doi.org/https://doi.org/10.1016/S0022-1694(03)00249-X, 2003.
Yong, L., Gao, H., Chang, Z., Guo, L., He, Z., He, X., and Fenicia, F.: Coupling stable isotopes and glacier mass balance reduces uncertainty in glacio-hydrological modelling, J. Hydrol. Reg. Stud., 64, 103312, https://doi.org/10.1016/j.ejrh.2026.103312, 2026.